Abstract

Pancorbo, Bruno Marco. Functional studies of ferritin 3-fold axis: effects of mutations near subunit interaction sites. (Under the direction of Dr. E. C. Theil)

Ferritin is an iron storage protein whose metabolic importance is reflected in its ubiquitousness in living organisms. Ferritin is a multi-subunit protein (24 subunits) and one of its most interesting features is its 3-dimensional structure: a sphere-like structure with a 4-3-2 symmetry that has a hollow interior where iron is stored. This 3-dimensional structure is highly conserved among ferritins of different living organisms even when the homology of the primary structure of the different ferritins is as low as 22%. Such a degree of structural conservation can only be interpreted as the result of a near perfect balanced between ferritin's structure and function.

Among the highly conserved residues are arginine 72 and aspartate 122 which form a salt bridge near the 3-fold interface. To study the importance of these residues in ferritin function, site-directed mutagenesis was used to disrupt and rescue this salt bridge. The properties of the mutants were tested and compared with those of the parent proteins.

The greatest difference between mutants and parent proteins was seen in the amount of iron each released. Mutants were found to release a greater percentage of their initial iron than the parents released. Some mutants also showed an increased rate of iron release over the parent proteins, but the effect of the mutation differed depending on the type of subunits used. Another finding was that disruption of the salt bridge caused some of the ferritin subunits to have an increase in volume which seems to correlate with the difference in iron uptake rates for the different ferritin mutants.

FUNCTIONAL STUDIES OF FERRITIN 3-FOLD AXIS: EFFECTS OF MUTATIONS NEAR SUBUNIT INTERACTION SITES

by

Bruno Marco Pancorbo

A thesis submitted to the Graduate Faculty of
North Carolina State University
in partial fulfillment of the
requirements for the Degree of
Master of Science

Biochemistry

Raleigh

2000

Approved by:

_____	_____
Chair of Advisory committee	Co-Chairman of Advisory committee

_____ _____ _____

Biography

Bruno Marco Pancorbo was born in Lima, Peru on January 27, 1971 to Mr. Augusto Pancorbo and Mrs. Belmira Rodriguez de Pancorbo. He came to the United States in May of 1989 where he completed his high school education in 1990. He entered Santa Fe Community College in 1991 and then transferred after 2 years to the University of Florida where he received his B.S. in Microbiology and Cell Science in 1994. From 1994 to 1996 he worked in the University of Florida Department of Pharmacology as a student assistant under the supervision of Dr. Thomas H. Maren. In August 1996 he entered the North Carolina State University Biochemistry program where he worked under the supervision of Dr. Elizabeth C. Theil.

Acknowledgments

I would like to express my sincere appreciation to my major professor, Dr. Elizabeth C. Theil, for the time and guidance she has provided. I would also like to express my gratitude for her understanding, patience and willingness to continue to as my major professor when we were on opposite coasts. I would especially like to thank Dr. Charles W. Carter (U.N.C. - Chapel Hill, Department of Biochemistry and Biophysics) for his advice, patience and bench space. Obtaining my degree would have been much more difficult if he had not agreed to my being housed in his lab for the last one and a half years. I would also like to thank the other members of my advisory committee, Dr. James Otvos, Dr. Dennis Brown and Dr. Hosni Hassan, for the advice and guidance they gave during my participation in this graduate program.

I would also like to thank Dr. Bill Small for the incredible amount of advice and help he has given. To Aixa Morales-Diaz I would say, “Muchas gracias!” She gave me whatever help I needed meeting the requirements of the graduate school.

I would like to thank my mother, Belmira de la Torre Ugarte, and my brother, Roberto V. Pancorbo for their support throughout the entirety of my education. I would also like to thank my late stepfather, Luis de la Torre Ugarte Barandiaran, for making so many things possible. I would also like to thank my sounding board, editor and girlfriend, Paula K. Knabb, for all the help and support she has given to me.

Table of Contents

Table of Contents (cont.)

List of Tables

List of Figures

Introduction

Ferritin is the protein which concentrates and stores iron in living organisms. It is composed of twenty-four subunits that form a sphere-like structure with a hollow core, 8 nm in diameter, where the iron is stored [1-3] . Three different kinds of subunits have been found in nature: M type, H type and L type. In terms of speed of iron uptake, M and H subunits form a class of fast ferritin, and L types are considered to be slow in iron uptake. The difference in iron uptake rate is more than one hundred fold. *In vivo*, animal ferritin is made by combining fast and slow subunits to form the final sphere [1, 4]. Ratios of fast and slow ferritin subunits vary among species and tissues, and the different ratios are thought to be the primary determining factor in the difference of iron uptake rates by different ferritins [2].

All ferritins have similar secondary, tertiary and quaternary structure [5-9]. They form five alpha helices which are designated helix A to helix E; A-D are the canonical four helix bundle. These helices are connected by short (about five amino acids) turns with the exception of the BC loop which is longer (24 residues).

Ferritins have a unique quaternary structure coincident with function. Each subunit has about 175 amino acids. Since only nine residues are highly conserved in all the known ferritin amino acid sequences, it is plausible that some of these conserved residues are important in ensuring the proper folding, assembly and function of ferritin. Two of these conserved residues, arginine 72 and aspartate 122, are found close to the 3-fold interface of the assembled ferritin protein. Although these two residues are far apart from each other as determined by the ferritin amino acid

sequence, closer inspection of the three dimensional structure of this region in protein crystals [5-9] reveals that these residues are positioned close together and form an intra-subunit salt bridge in all types of subunits. Because aspartate 122 is conserved in all ferritin sequences known to date and arginine 72 is conserved in thirty-three of the thirty-four known sequences, the importance of this putative salt bridge in the assembly and function of ferritin was studied.

Experimental Procedure

Mutagenesis

Site directed mutagenesis of frog ferritin H subunits and M subunits were performed using the Chameleon double-stranded site directed mutagenesis kit (Promega). The oligonucleotides H R72D (5'GGACAATGCGACCCCCATCTTTGTTCTGATCC3'), H R72DD122R (5'CCAAGAAGTCACACAGATGGGGGCGAACCTTGTCAGATCC3'), M R72D (5'GGACAACACGTCCCCCATCCTTGTTTTGATATTTCATG3') and M R72DD122R (5'GGAAATCACACAGATGGGGGCGAACTTTGTCCGTGGCC3') were used as mutagenic primers. For the double mutants, the mutagenic primers were used sequentially to obtain the desired mutation. The pET 9a (Novagen) plasmid that confers kanamycin resistance was used to subclone the sequences of H-wt, H R72D and H R72DD122R, and the pET3a (Novagen) that confers ampicillin resistance was used for M-wt and M R72D. *E. coli* (BL21D(e3)) was used as the expression system. Due to low expression of H R72D and H 72DD122R ferritins, transformed cells were co-transfection with pET 3a because earlier findings in our lab showed that the expression of some ferritin mutants is improved by the use of multiple antibiotics during incubation. M R72D was also co-transfected with pET9a to increase protein expression.

Expression and purification of wild type and recombinant ferritin proteins

Bacterial cultures were grown as described in previously [10-12] with the following modifications for H R72D, H R72DD122R and M R72D: standard 500 ml medium in 2L flask cultures gave very little soluble protein as determined by SDS-PAGE, therefore, smaller culture volumes of 100 ml medium in 250 ml flask were used to increase the yield of soluble protein expressed. The cultures were grown at 26 ^{o}C because it had been shown in earlier experiments that incubation at this temperature increased the expression of soluble ferritin protein. Growth time was 26 hours. For all of the proteins, induction time with 0.4 M IPTG was limited to 2.5 hours to minimize inclusion body formation.

Cell cultures were then spun in 1L bottles for 40 minutes at 5000 rpm at 4 ^{o}C. Pellets were then collected and washed with 20 mM Bis-Tris Propane, 1M NaCl, 1mM Betaine pH 7.6 twice at a ratio of 6 ml wash solution per gram of cells in 50 ml Oakridge tubes. Cell were spun at 8000 rpm (SA Sorbal) following the first wash and at 13000 rpm (SA Sorbal) following the second wash. Resulting pellets were then sonicated 3 times for a period of 30 seconds with 1 minute intervals between sonication steps. The sonicated solution was then spun at 13000 rpm (SA Sorbal) for 10 minutes, and the supernatant was then heated to 75 ^{o}C for 15 minutes and spun at 13000 rpm (SA Sorbal) for 10 minutes. The supernatant was then collected and mixed with ammonium sulfate (0.45gm/ml) until it was completely dissolved. Following an incubation period of at least 2 hours at 4 ^{o}C, the solution was spun at 16000 rpm (SA Sorbal) for 40 minutes. The supernatant was discarded and the pellet resuspended in 20 mM Bis Tris Propane, 0.09 M NaCl, 1mM Betaine pH

7.6 and dialyzed against the same buffer overnight. Following dialysis, the solution was filter sterilized (0.2µ) and applied to an ion exchange column (Q-Sepharose Pharmacia (c)). The fractions were analyzed by SDS-PAGE and absorption at 280 nm. Pooled fractions were then mixed with ammonium sulfate (0.45g/ml) and incubated at 4 ^{o}C overnight. The protein was sedimented by centrifugation at 16000 rpm (SA rotor) for 40 minutes, and the pellet was resuspended in 50 mM MOPS, 0,2M NaCl, pH7.6 and dialyzed twice against three hundred volumes of the same buffer. The first dialysis was overnight, and the second was for a period of 4 hours.

The R72DD122R mutation was made in the M subunit as well. However, this protein could not be successfully purified due to inclusion bodies.

Gel filtration experiments

A sephacryl S300 (Pharmacia) gel filtration analytical column was used for all the gel filtration experiments. The column was attached to a perfusion chromatography system (BioCAD Sprint), and the temperature of the column was controlled using a water pump. To ensure proper temperature stabilization of the column, water was run over the column at the desired temperature overnight. The column was equilibrated with 2 column volumes of 50 mM MOPS, 0.2M NaCl pH 7.6. The flow rate was 0.8 ml/min throughout, and 0.5 ml of sample were injected. In general, the amount of protein applied to the column was 1.4 mg. Elution times were determined using the BioCAD Sprint system software and absorbance at 280 nm.

Iron uptake - initial peroxidiferric complex (A 650 nm)

Ferritin samples stored in 0.2 M NaCl, 0.05M MOPS pH 7.0 were mixed with 1M MOPS pH7.0, 2M NaCl and H_20 to a final concentration of 2.0 mg/ml ferritin, 0.2M MOPS pH 7.0 and 0.2M NaCl. To test the formation of the peroxidiferric complex using the stop flow spectrophotometer, one ml of the protein sample was placed in the left chamber and 1 ml of a solution made by mixing 1482 µl of 0.2 M NaCl, 1mM HCl with 18.8 µl of 16 mM FeSO4 $7H_2O$, 0.2 M NaCl, 1 mM HCl was placed in the right chamber. Final Fe/ferritin ratio after mixing was 48. The formation of the peroxidiferric complex was followed by measuring the absorption of the sample at 650 nm. The peroxidiferric formation rates were calculated from the slope of the formation curves by linear regression.

Iron uptake - polynuclear iron (A 350 nm)

Ferritin samples stored in 0.2 M NaCl, 0.05M MOPS pH 7.0 were mixed with 1M MOPS pH 7.0, 2M NaCl and H_20 to a final concentration of 1.1 mg/ml ferritin, 0.2M MOPS pH 7.0 and 0.2M NaCl (solution A). Nine hundred µl of this sample was used as the blank. Formation of the iron core was monitored by following the absorption at 350 nm after the sample was mixed with solution B . Solution B was prepared immediately before use by mixing 27.5 mg of $FeSO_4$ with 800 µl of 2.5 M NaCl, 100 µl of 0.1 M HCl and enough H_2O to achieve a final volume of 10 ml. After mixing, the Fe to iron ratio was 480 Fe/ ferritin molecule.

Iron release - iron reduction (A 522 nm)

Ferritin samples stored in 0.2 M NaCl, 0.05M MOPS pH 7.0 were mixed with 1M MOPS pH7.0, 2M NaCl and H_20 to a final concentration of 1.1 mg/ml ferritin, 0.2M MOPS pH 7.0 and 0.2M

NaCl. Four hundred and eighty Fe/ferritin cores were made by mixing 0.9 ml of a 1.1 mg/ml ferritin, 0.2M MOPS pH 7.0 and 0.2M NaCl sample with 0.1 ml of 9.6 mM $FeSO_4H_2O$ (in 1 mM HCl, 0.2M NaCl) and incubated at room temperature for 2 hours and then at 4 ^oC overnight. A solution was made by mixing 100 µl 25 mM NADH, 100 µl of 25 mM FMN, 100 µl 1M MOPS pH 7.0, 100 µl 2M NaCl and 500 µl of H_2O in a plastic 1 ml cuvette. The NADH and FMN solutions were prepared immediately before use. To induce iron release, 100 µl of the protein solution was quicky mixed with the solution in the cuvette to start the reaction.

Iron release was measured by the formation of a bypiridyl-Fe(II) complex which was followed by the change in absorption at 522 nm using an HP diode array spectrophotometer. Absorbance measurements were taken every 5 seconds for the first minute, every 30 seconds for the next 5 minutes and then every 5 minutes until the end of the experiment, usually 90 minutes. The iron release rates were determined by calculating the slope of the curve for absorbance during the first 40 seconds of the reaction.

Results

Effects of mutations on iron uptake rates

Mutation at the 3-fold interface had different effects on the rate of iron uptake depending on the sequence of the ferritin subunit (Fig. 3.) Mutation in the frog H subunit showed a decrease in the iron uptake rate. The biggest difference was produced by the H R72D mutant that showed a 3.7 fold decrease (0.77 +/- 0.34 ÄAu/sec) in its iron uptake rate compared to that of the wild type H (2.9 +/- 1.4 ÄAu/sec). The double mutant, H R72DD122R, also showed a decrease in its iron

uptake rate (1.24 +/- 0.44 ÄAu/sec), but this decrease was less than that off H R72D. In contrast, mutations in the M ferritin subunits did not cause any significantly different results in iron uptake rate for the M-wt (1.68 +/- 0.38 ÄAu/sec) and M R72D (2.0 +/- 0.5 ÄAu/sec.)

Effects of mutations on the iron release rates

Disruption of the putative salt bridge had different effects in the iron release rates depending on the type of ferritin subunit studied. The different iron release rates for the wild type and mutant ferritins are shown in figure 4. The largest change on the iron release rate was seen in the double mutant, H R72DD122R, which showed a 4.3-fold increase in its iron release rate (6.75 $10^{-}3$) compared to the iron release rate of the wild type H (1.57 $10^{-}3$). The single mutant, H R72D, also showed an increase of 2.2 fold (3.69 $10^{-}3$) over the wild type protein. In contrast, the M R72D mutant showed a very small decrease in its iron release rate compared to that of the wild type M (1.30 $10^{-}3$ and 1.76 $10^{-}3$, respectively.)

Effects of mutations on amount of iron released

As figure 5 shows, disruption of the putative salt bridge caused an increase in the amount of iron released in both H and M types of ferritin. Both H mutants, H R72D and H R2DD122R, exhibited an increase of more than 58% in the amount of iron released after 10 minutes. After this time H R72D released 77.3% while H R72DD122R released 77.4% of its initial iron atoms, and the H-wt released only 48.8 %. This increase is not transient and causes these two mutants to reach higher iron release percentage than the wild type even after longer incubation times. Figure 5B depicts the percentage of iron released after 40 minutes. At this time these mutants and the wild type

showed a very small increase in the percentage of iron atoms released, but the differences in iron released by the H mutants and H-wt was still high. After 40 minutes, the H R72D released 82% while H R72DD122 released 81% of its total iron content compared to only 60 % for the wild type H.

Even more striking results are seen in the M mutants. Although the M subunit does not normally reach iron release amounts higher than 30 % when incubated with 480 Fe/ferritin, MR72D mutants attained an iron release amount closer to that of the H wild type after 10 minutes and even higher after 40 minutes. As figure 5A shows, after 10 minutes, M R72D had released about 42.8 % of its iron content compared to only 24 % iron released by the wild type M. This is more that a 1.7 fold increase in iron release over the wild type M. As in the case of the H mutants this increase is not transient and continues to increase over time. After 40 minutes the M R72D released almost 79 % percent of its total iron while M-wt released 30 %. This increase in amount of iron released by the M R72D is 2.3-fold higher than the amount of iron released by M-wt.

Effect of mutations on gel filtration elution times

Because ferritin is a twenty-fourmer, mutation in one of the subunits will be amplified in the assembled protein. To analyze the possible effect on the volume of the proteins due to the mutations at the 3-fold interface, gel filtration experiments were performed using an analytical grade gel filtration column (Table 1).

Mutation in the H subunits revealed marked differences in the elution time of the protein. Table 3 shows a summary of the elution times at different temperatures. The largest difference from wild type was observed in the elution time of H R72D with a mean elution time of 64.30 +/- 0.28 min at 23 ^{o}C. H R72DD122R had an mean elution time of 66.75 +/- 0.07, and the H-wt had a mean elution time of 67.75 +/- 0.07 min. In contrast, mutations in the M class of subunits did not show any significant difference between the mutant and wild type (65.40 +/- 0.51 for the M R72D and 65.70 +/- 0.29 for M-wt). At 10 ^{o}C a very small difference in elution time was observed for MR72D and the wild type M. At 10 ^{o}C and 45.5 ^{o}C all the elution times changed as expected, decreasing and increasing as the protein volumes condensed and expanded respectively. The difference in the elution time of the wild type and the mutant proteins decreased slightly as the temperature was increased.

Discussion

Mutations at the 3-fold interface and the effects on protein volume

From the results of the gel filtration experiments, it is clear that the R72D and R72DD122R mutations in the H ferritins showed an increase in volume compared to the volume of the wild type protein (Fig. 7 A, B, C.) As determined by the elution times of the different mutants, the larger increase in volume was seen in the single mutant, H R72D, followed by the double mutant, H R72DD122R. In contrast to these results, the R72D mutation in the M subunit did not cause a marked difference from the wild type M in regards to volume. The greatest difference in elution times between mutants and wild type subunits was seen at 10 ^{o}C. However, at this temperature

the difference in the elution times of M R72D and M-wt is only 0.6 % which is just above its standard deviation value (0.247).

It is difficult to determine the possible reason(s) for the difference in behavior of the mutants from the three dimensional structure because the tertiary and quaternary structures of H and M ferritins are identical [7, 8]. However, the number of interactions between the 3-fold terminus of the AB helix bundle and the terminus of the CD helix may not be the same in both the H and M subunits. While in the H ferritins it seems that the primary interaction between these two bundles is through the R72-D122 salt bridge, in the M ferritin subunits there is an additional hydrophobic interaction between tyrosine 68 and phenylalanine 128 (Fig. 8.) The stacking of the aromatic rings of these residues might serve as an additional lock to secure the bundles in place in the M subunit. While most ferritins have a tyrosine or a leucine at position 68 (as is the case of human H ferritin), frog H ferritin has an aspartate and thus lacks the extra stability imparted by the hydrophobic interaction between Y68-F128. Additionally, using the program ProCam [13] designed to identify intra-subunits hydrophobic interactions, it is possible to determine the difference in the number of hydrophobic interactions found in 3 different ferritin subunits: frog M and L ferritin and human H ferritin. Figure 9 shows the different hydrophobic interactions for human H and frog M ferritin. This program requires the use of the 3 dimensional structure of the protein. This data is not available for frog H ferritin at this time, so the human H ferritin sequence was used for this comparison [14]. Although the sequence homology between the human H ferritin sequence and frog H ferritin is lower (86 %) than the sequence homology between frog H ferritin and frog M ferritin (93 %), the homology at the residues directly involved in the hydrophobic interactions is

higher between the human H and frog H ferritins (72 %) compared to that of the frog H and frog M ferritins (63 %) Therefore, the probable number of hydrophobic interactions in frog H ferritin can be extrapolated from analysis of the human H ferritin. The number of interactions for human H, frog M and frog L ferritin is summarized in Table 3.

From this table, is it clear that the number of hydrophobic interactions within the frog M subunits is much larger than that in the frog L and human H subunits. Of the residues predicted to be involved in the hydrophobic interactions in human H ferritin all are identical to the corresponding residues in frog H ferritin except at 2 positions. Human H ferritin has a glutamine at position 19 while frog H ferritin has a methionine at this position. In addition, human H ferritin has a leucine at position 68 while frog H ferritin has an aspartate at this position. This increase in stability due to the higher number of hydrophobic interactions in the frog M ferritin could explain the differential effect in size due to the R72D mutation in the H and M subunits.

Iron release and the 3-fold interface

Although there has been extensive research into the mechanism of iron uptake by ferritin, current understanding of the mechanism of iron release by ferritin is limited. First indications are that the 3-fold axis is involved. From experiments by Takagi *et al* [15] it was shown that there was an increase in the iron release rate which correlates with the disruption of the end of the C helix and the beginning of the D helix which was caused by the substitution of a conserved leucine residue by a proline. How these changes in the 3-fold interface of ferritin affect iron release is not known. In a similar fashion, disruption of the salt bridge between arginine 72 and aspartate 122 by the

R72D and R72DD122 mutations increases their iron release rate. A closer look at the position of this salt bridge with respect to the L134P mutation can be seen in figure 6. While the L134P mutation disrupts the C terminus of the C alpha helix and the N terminus of the D alpha helix, disruption of the R72-D122 salt bridge would remove an anchor that connects the 3-fold end of the AB alpha helix bundle to the CD alpha helix bundle. The end result of both mutations, L134P and R72D, could be very similar from a structural point view, increased flexibility at the 3-fold interface. While direct determination of the structure of the H R72D mutant is not yet available, gel filtration studies show that an increase in the volume of the protein can be achieved by disruption of the R72D salt bridge in the H type of subunits, supporting the hypothesis of increase flexibility.

As stated earlier the double mutant, H R72DD122R, shows an even higher increase in its iron release rate compared to that of the H R72 mutant. From this result and from its other properties, it is clear that the double mutant did not fully rescue the salt bridge as predicted.

In contrast, the M R72D mutation did not show a significant increase in iron release rate in the M subunits. This result seems strange due to the fact that the M R72D mutant releases more iron than the wild type M after 10 and 40 minutes. The cause of this result is not known, but an explanation for the difference observed in iron release amount and the difference in volume observed in the gel filtration studies of the H and M proteins could be due to a specific property of the arginine 72. As stated earlier, the difference in volume was seen only in the H mutants but not in the M mutant. At the same time, there is a large difference in the percentage of iron

released by the mutants, especially by MR72D. If the R72 residue is involved directly in the iron release pathway, its absence would directly affect the iron release process as is seen in both the H mutants and the M mutant.

Iron uptake and the 3-fold interface

Iron is believed to enter ferritin through the 3-fold interface [16-18]. There is a considerable amount of information on the effect that mutations in the 3-fold interface [19-26] have on the iron uptake rate of ferritin. There is solid evidence that several residues in the center of the double helix bundle of the ferritin subunit, E23, E58, H61, E103 and Q 137 which together compose the ferroxidase center, participate in the initial steps of the iron uptake [3, 27-29] , but the direct importance of the 3-fold interface in the iron uptake mechanism is not known. Even though the salt bridge between R72 and D122 is as far away from the center of the subunits as possible (about 24 Å), its disruption affects the iron uptake rates of H subunits but produces only a very small difference in the iron uptake rate of the mutant M subunit (Figure 3.) One explanation for the differential effect of the R72D mutation on H and M subunits could be explained by a difference in the microenviroment of the ferroxidase center. Frog H (and also human H) have only one ExxH motif (E58 H61) which works in conjunction with E23, E 103 and Q137. In contrast, frog M ferritin has this same binding motif but also has an additional binding motif formed by Q137xxD140 which gives this protein different reaction kinetics from the H ferritin subunits. The additional QxxD motif in the frog M subunits is thought to increase stabilization of the initial diferric complex which is a precursor of mineralization [7] and might have some biological

relevance [30]. This increase in stability found in the M subunits could be the reason for the different iron uptake properties seen in M R72D and H R72D.

Another explanation for the difference in iron uptake by the R72D mutation in H and M frog ferritins can be the result of the differential effect of the disruption of the salt bridge in H and M ferritins. From the gel filtration experiments it was shown that the H ferritins increase in volume due to the disruption of the salt bridge but that the M subunits do not. A relationship between iron uptake rate and gel filtration elution time can be seen in figure 10. If we think of the two alpha helix bundles as two separate units that are connected by inter-bundle interactions, disruption of the salt bridge in the H subunits will cause these 2 bundles to have much more flexibility which will be manifested by a separation and lateral movement of the two helix bundles with respect to one another. This movement would result in a separation of the center residues found in both bundles thereby decreasing their optimal distance needed for iron uptake. Thus a separation of the AB and CD bundles would result in a decrease in iron uptake properties of the protein. This increased flexibility and separation of the AB and CD bundle caused by disruption of the salt bridge would not be expected to be as dramatic in the M subunit since it is locked more securely in place by additional hydrophobic interactions not present in the H subunits. This would explain the differential effect on iron uptake rate that is produced by the disruption of the R72-D122 salt bridge. Another piece of information that supports this theory is the findings of research done on an L134P mutation in the frog H subunit. Just like the H R72D mutant, the iron uptake rate of H L134P is considerably decreased compared to that of the wild type. While the H R72D mutant directly disrupts the salt bridge, one of the anchors between the AB and CD bundle, the L134P

mutation disrupts a large alpha helix segment, from L 110 to L 134. Because the electron density map [15] in the region of the D122 residue is very disorganized, it is likely that the L134P mutation also disrupts the R72-D122 salt bridge as well, thus producing an effect similar to that of the H R72D mutation.

Conclusions

It is clear that disruption of the salt-bridge between R72 and D122 had different effects depending on the type of ferritin subunit used. Although the 3-dimensional structure of H and M ferritin is very similar, the microenviroment of these proteins can be quite different. These differences in microenviroment give the ferritin subunits different properties which no doubt nature has used to its advantage. The effects of the disruption of the salt bridge are influenced by the different microenvironments of the H and M subunits, therefore, the net effects are different for the two types of subunits.

Other properties affected by the disruption of the salt-bridge are the iron uptake rate, iron release rate and amount of iron released. These changes in ferritin protein function due to the mutation of only one residue emphasize the importance of the salt bridge which was inferred from the conservation seen in the protein sequence.

While it is difficult to give concrete reason for the various changes in ferritin properties due to the disruption of the salt-bridge, there seemed to be two possible explanations for the differences. First, the increase in volume seen in the H ferritin could be directly related to the difference in iron uptake rates. This increase in volume could be due to the change in the optimal distance of the residues directly involved in the iron oxidation pathway. This idea is also supported by the fact that the M ferritin subunits do not show significant differences in their iron uptake properties nor in their volume. Another explanation for this difference is the fact the M subunits have an

additional iron binding motif not found in H subunits that increases the stability of the initial iron/ferritin binding.

Second, the R72 residue or the whole salt bridge could be directly involved somehow in the iron release pathway. This conclusion is supported by the fact all the R72D mutants in H and M frog ferritin show an increase in the amount of iron released irrespective of changes in volume of the protein. This observation is also partially supported by the changes in the L134P mutant in which the R72 residue is present but in a state of high disorganization.

References

1. Harrison, P.M., and Arosio, P., *The ferritins: molecular properties, iron storage function and cellular regulation.* Biochim. et Biophys. Acta, 1996. **1275**: p. 161-203.
2. Waldo, G.S., and Theil, E. C., *Comprenhenseve Supramolecualar Chemistry, ,* K.S. Suslick, Editor. 1996. p. 65-89.
3. Pereira, A.S., Tavares, P., Lloyd, S. G., Danger, D., Edmonson, D. E., Theil, E. C., and Huynh, B. H., *Rapid and Parallel formation of Fe (III) Multimer, including a Trimer, during H-Type Subunit Ferrtin Mineralization.* Biochemistry, 1997. **36**: p. 7917-7927.
4. Fox, B.G., Shanklin, J., Ai, J., Loehr, T.M. and Sanders-Loehr, J., *Resonance Raman evidence for an Fe-O-Fe center in stearoyl-ACP desaturase. Primary sequence identity with other diiron-oxo proteins.* Biochemistry, 1994. **33**: p. 12776-12786.
5. Forlow, F., Kalb, A. J., Yariv, Joseph, *Structure of a unique twofold symetry haem-binding site.* Strucutural Biology, 1994. **1**(7): p. 453-460.
6. Galloid, B., Langlois d'Estaintot, B., Michaux, M., Dautant, A., Granier, T., Precigoux, G., Soruco, J-A., Roland, F., Chavas-Alva, O., Herbas, A., and Crichton, R., R., *X-Ray structure of recombinant horse L-chain apoferritin at 2.0 A resolution: implications for stability and function.* JBCI, 1997. **2**: p. 360-367.
7. Ha, Y., Shi, D., Small, W., Theil, E. C., Allewell, N. M., *Crystal Structure of Bullfrog M Ferritin at 2.8 A Resolution: Analysis of Subunit Interactions and Direct Visualization of a Binuclear Metal Center.* J Biol Inorg Chem., 1999. **4**(3): p. 243-56.

8. Lawson, D.M., Artymiuk, P. J., Yewdall, S. J., Smith, J. M. A., Livingstone, J. C., Treffry, A., Luzzago, A., Levi, S., Arosio, P., Cesarini, G., Thomas, C. D., Shaw, W. V., Harrison, P. M., *Solving the Structure of Human H Ferritin by Genetically Engineering Intermolecular Crystal Contacts.* Nature, 1991. **349**: p. 541.

9. Trikha, J., Theil, E. C., Allewell, N. M., *High Resolution Crystal Structures of Amphibian Red-Cell L Ferritin: Potential Roles for Structural Plasticity and Solvation in Function.* J. Mol. Biol., 1995. **248**: p. 949.

10. Fetter, J., Cohen, J., Danger, D., Sanders-Loehr, J., and Theil, E. C., J. Biol., *The influence of conserved tyrosine 30 and tissue-dependent differences in sequence on ferritin function: use of blue and purple Fe(III) species as reporters of ferroxidation.* Inorg. Chem, 1997. **2**: p. 652-661.

11. Waldo, G.S., and Theil, E. C., *Formation of iron(III)-tyrosinate is the fastest reaction observed in ferritin.* Biochemistry, 1993. **32**: p. 796-798.

12. Waldo, G.S., Ling, J., Sanders-Loehr, J., and Theil. E. C., *Formation of an Fe(III)-Tyrodinate complex during Biomineralization of H-subunit Ferritin.* Science, 1993. **259**: p. 796-789.

13. Stephen A. Cammer, C.C., Iosif Vaisman, Alex Tropsha., *ProCam*, . 1998: UNC Chapel Hill.

14. Hempstead, P.D., Yewdall, S. J., Fernie, A. R., Lawson, D. M., Artymiuk, P. J., Rice, D. W., Ford, G. C., Harrison, P. M., *Comparison of the Three-Dimensional Structures of Recombinant Human H and Horse L Ferritins at High Resolution.* J. MOL. BIOL., 1997. **268**: p. 424.

15. Takagi, H., Shi, D., Ha, Y., Allewell, N. M., and Theil, E. C., *Localized Unfolding at the Junction of Three Ferritin Subunits.* The Journal of Biological Chemistry, 1998. **273**(30): p. 18685-18688.

16. Lee, M., Arosio, P., Cozzi, A. and Chasteen, N. D., *Identification of the EPR-active iron-nitrosyl complexes in mammalian ferritins.* Biochemistry, 1994. **33**: p. 3679-3787.

17. Treffry, A., Bauminger, E.R., Hechel, D., Hodson, N. W., Nowik, E., Yewdall, S.G., and Harrison, P. M., *Defining the roles of the threefold channels in iron uptake, iron oxidation and iron-core formation in ferritin: a study aided by site-directed mutagenesis.* Biochem J., 1993. **296**: p. 721-728.

18. Lawson, D.M., Treffry, A., Arthmiuk , P.G., Harrison, P. M., Yewdall, S. J., Luzzago, A., Cesareni, G., Levi, S., and Arosio, P., *Identification of the ferroxidase centre in ferritin.* FEBS Letters., 1989. **254**: p. 207-210.

19. Wardeska, j.G., Viglione, B., and Chasteen, N. D., *Metal ion complexes of apoferritin. Evidence for initial binding in the hydrophilic channels.* J.Biol. Chem, 1986. **261**: p. 6677-6683.

20. Harrison, P.M., Treffry, A., and Lilley, T. H., *Ferritin as an iron-storage protein: mechanisms of iron uptake.* Biochemistry, 1986. **27**: p. 287-293.

21. Stefanini, S., Desideri, A., Vecchini, P., Drakenberg, T., and Chiancone, E., *Identification of the iron entry channels in apoferritin. Chemical modification and spectroscopic studies.* Biochemistry, 1989. **378-382**.

22. Treffry, A., Harrison, P. M., Luzzago, A., ans Cesarini, G., *Recombinant H-chain ferritins: effects of changes in the 3-fold channels.* FEBS Letter, 1989. **287**: p. 268-272.

23. Desideri, A., Stefanini, S., Polizio, F., Perruzzelli, R. and Chiancone, E., *Iron entry route in horse spleen apoferritin. Involvement of the three-fold channels as probed by selective*

reaction of cysteine-126 with the spin label 4-maleimido-tempo. FEBS letter., 1991. **287**(10-14).

24. Sun, S., Arosio, P., Levi, S., Chasteen, N.D., *Ferroxidase kinetics of human liver apoferritin, recombinant H-chain apoferritin, and site-directed mutants.* Biochemistry, 1993. **32**: p. 9362-9369.
25. Yablonski, M.J., Theil, E.C., *A possible role for the conserved trimer interface of ferritin in iron incorporation.* Biochemistry, 1992. **31**: p. 9680-9684.
26. Macara, I.G., Hoy,T.G., Harrison, P.M. Biochem. J., *The formation of ferritin from apoferritin. Inhibition and metal ion-binding studies. Biochem J.*, **1973**. ***135***: p. 785-789.
27. Pereira, A.S., Small, W., Krebs, C., Tavares, P., Edmonson, D. E., Theil, E. C., and Huynuh, B. H, *Direct Spectroscopic and Kinetic Evidence for the Involvement of a Peroxodiferric Intermediate during the Ferroxidase Reaction in Fast Ferritin Mineralization.* Biochemistry, 1998. **37**(28): p. 9871-9876.
28. Moenne-Loccoz, P., Krebs, C., Herlihy, K., Edmonsons, D. and E., Theil, E. C., *The Ferroxidase reaction of Ferritin Reveals a Diferric u-1,2 Bridging Peroxide Intermediate in Common with Other O_2 Activating Non-Heme Diiron Proteins.* Biochemistry, 1999. **38**: p. 5290-5295.
29. Treffry, A., Zhao, Z., Quail, M. A., Guest, J. R., and Harrison, P. M., *Dinuclear Center of Ferritin: Studies of Iron Binding and Oxidation Show Differences in the Two Iron Sites.* Biochemistry, 1997. **36**(2): p. 432-441.
30. Theil, E.C., Small, W. S., He, L., Tipton, A.R., Danger, D., *The Ferritin Iron Entry and Exit Problem.* Inorganica Chemical Acta, In press.

Table 1. Initial iron uptake rates

Protein	Rate @ 350 nm (Au/sec 10^{-2})
H-wt	2.9 +/-1.4
H R72D	0.77 +/- 0.34
H R72DD122R	1.24+/- 0.44
M-wt	1.68 +/- 0.38
M R72D	2.0 +/- 0.5

Table 1. Iron uptake rate (formation of polynuclear iron clusters) for different recombinant apoferritins (initial Fe/ferritin concentration less than 15 Fe/ferritin). Initial iron uptake rates were determined by mixing 1mg/ml ferritin solution with a ferrous sulfate solution to a ratio of 480 Fe/ferritin. Absorbance measurements at 350 nm were made every 5 seconds for 5 minutes, and the iron uptake rate was determined by calculating the slope of the curve for the first 30 seconds. Shown rates are the average of at least 3 different protein batches of each ferritin protein. Errors for the initial rates are the standard deviation of the mean.

Table 2. Iron release rates

Protein	Rate @ 522 nm (Au/sec $10^{-}3$)
H-wt	1.57 +/- 0.26
H R72D	3.69 +/- 0.61
H R72DD122R	6.75 +/- 0.89
M-wt	1.76 +/- 0.32
M R72D	1.30 +/- 0.62.

Table 2. Iron release rates for different recombinant apoferritins. Ferritins were preincubated with a ferrous sulfate solution so the final iron to protein ratio was 480. Reduced iron was trapped by the formation of a bipyridyl complex whose formation was followed at 522 nm. Absorption measurements were taken every 5 second for the first 2 minutes, and the iron release rates were determined by calculating the slope of the curve for the first 50 second of the reaction.

Table 3. Elution times as a function of temperature

Protein	Temperature (ºC)		
	10	23	45
H Wt	66.47 +/- 0.13	67.75 +/- 0.07	69.45 +/- 0.10
H R72D	63.15 +/- 0.07	64.30 +/- 0.28	66.30 +/- 0.57
H R72DD122R	64.87 +/- 0.14	66.75 +/- 0.07	68.21 +/- 0.30
M Wt	64.29 +/- 0.24	65.70 +/- 0.29	67.52 +/- 0.26
M R72D	63.93 +/- 0.22.	65.40 +/- 0.51	67.47 +/- 0.13

Table 3. Gel filtration elution times at different temperatures for several recombinant apoferritins. Error of the elution time (min) is the standard deviation of the mean.

Table 4. Hydrophobic interaction in the 3-fold end terminus of the AB-CD ferritin helix bundle

Ferritin Proteins		
Frog M	Human H	Frog L
C12-V16-L113-L125	Y8-I16-L68-L125	F8-L16-Y68-M125
V16-F65–Y68-L125	I16-L68-L125-F128	C12-L16-L113-M125
Y8-V16-Y68-L125	I16-L113-L125-I129	L16-L113-M125-L129
V16-L133-L125-L129	I16-L65-L68-F128	L16-Y68-M125-F128
V16-F65-L125-L129	I16-L65-L113-I129	L16-L65-L113-L129
V16-F65-L113-L129		L16-L65-Y68-F128
V16-M19-F65-L113		L65-L110-L129-Y133
M19-F65-L113-L129		
M19-L110-L113-L129		
M19-F65-L110-L129		
F65-L110-L129-Y133		
M19-F65-L110-Y133		

Table 4. Intra-subunit hydrophobic interactions at the 3-fold terminus of the AB-CD alpha helix bundle in recombinant frog M and human H ferritins. The hydrophobic interactions were determined using the program ProCam (1998 Stephen A. Cammer, Charles Carter, Iosif Vaisman, Alex Tropsha: UNC Chapel Hill.)

Supramolecular Ferritin Structure

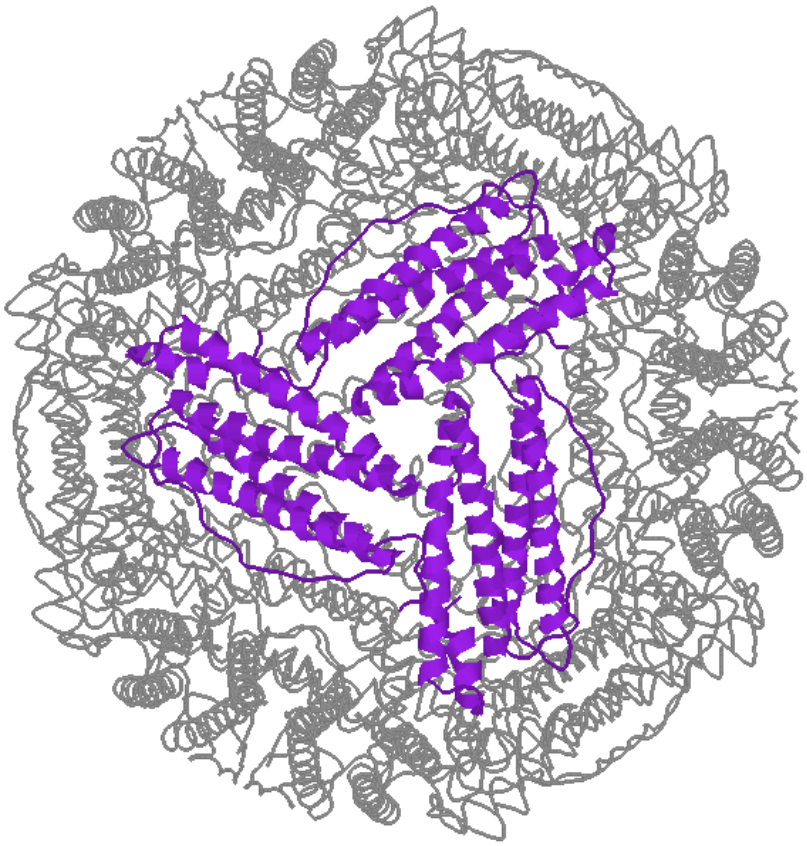

Fig 1. Frog M ferritin 24 subunits in a 432 symmetry viewed down the 3-fold axis. Purple ribbon shows the packing of 3 ferritin subunits to form the 3-fold interface. In gray is shown an á-Carbon trace drawing of the other 21 subunits. (Drawing produced by Rasmol.)

Salt-bridge between R72-D122 in the 3-fold interface of frog M ferritin

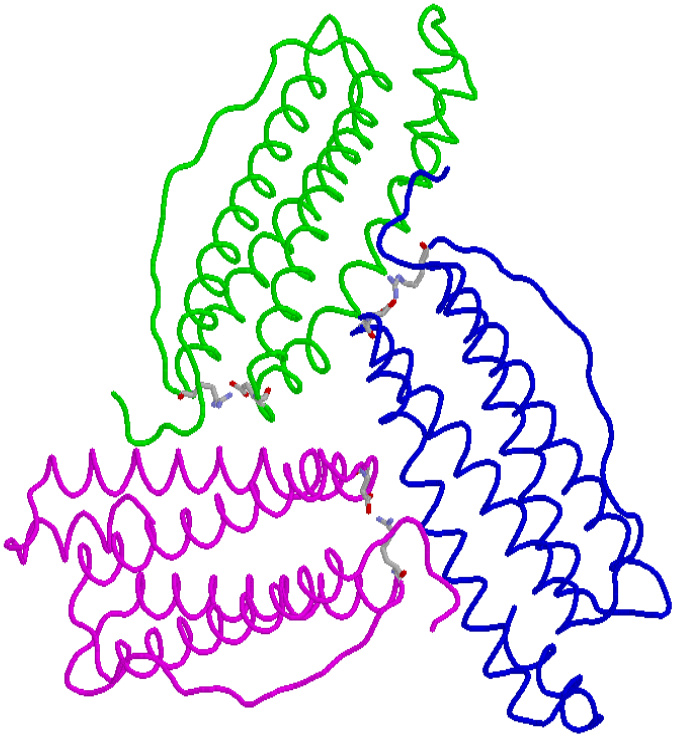

Figure 2. Trace drawing of frog ferritin 3-fold axis and the salt bridge between R72 and D122. Trimer interface showing the position on the inter-subunits salt bridge between arginine 72 and aspartate 122. (Drawing produced by Rasmol.)

Iron uptake rates

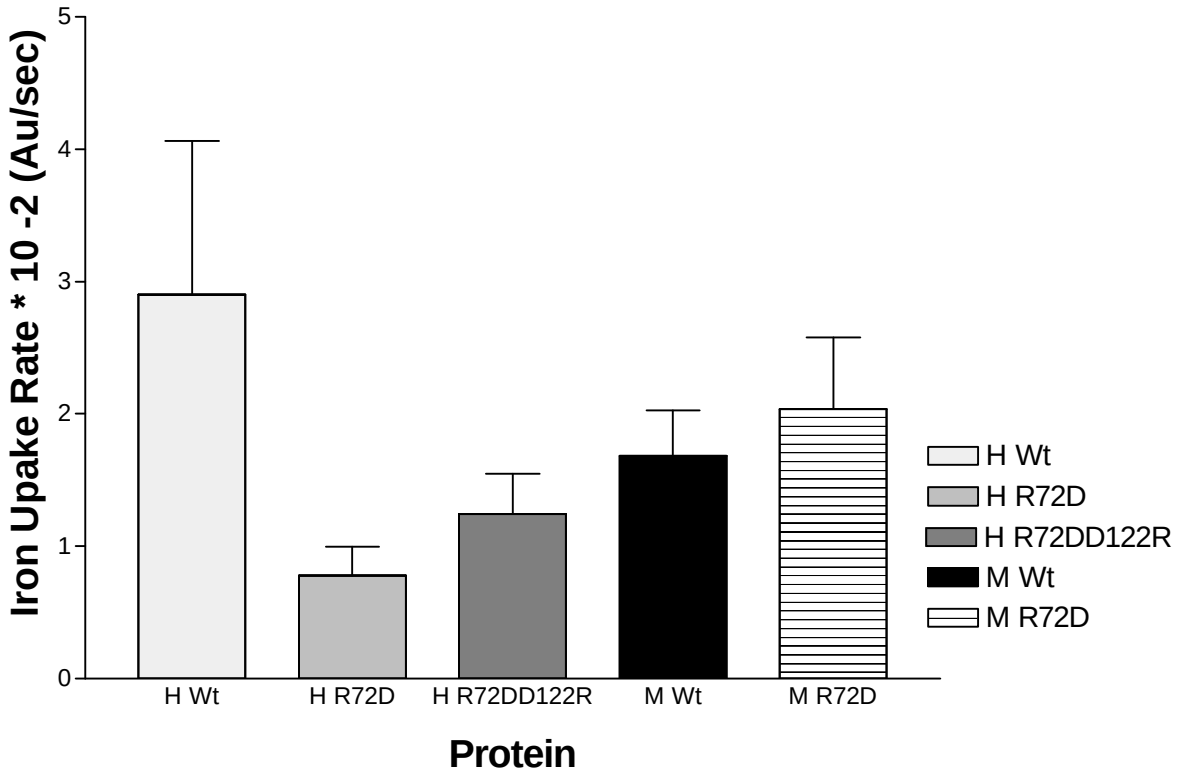

Fig 3. Iron uptake rates for various recombinant apoferritins. The error of the initial rates (ÄAu/sec) is the standard deviation of the mean. H-wt, 2.9 +/- 1.16; H R72D, 0.77 +/- 0.22 ; H R72DD122R, 1.24 +/- 0.303; M-wt, 1.68 +/- 0.34; M R72D 2.0 +/- 0.53.

Iron release rates

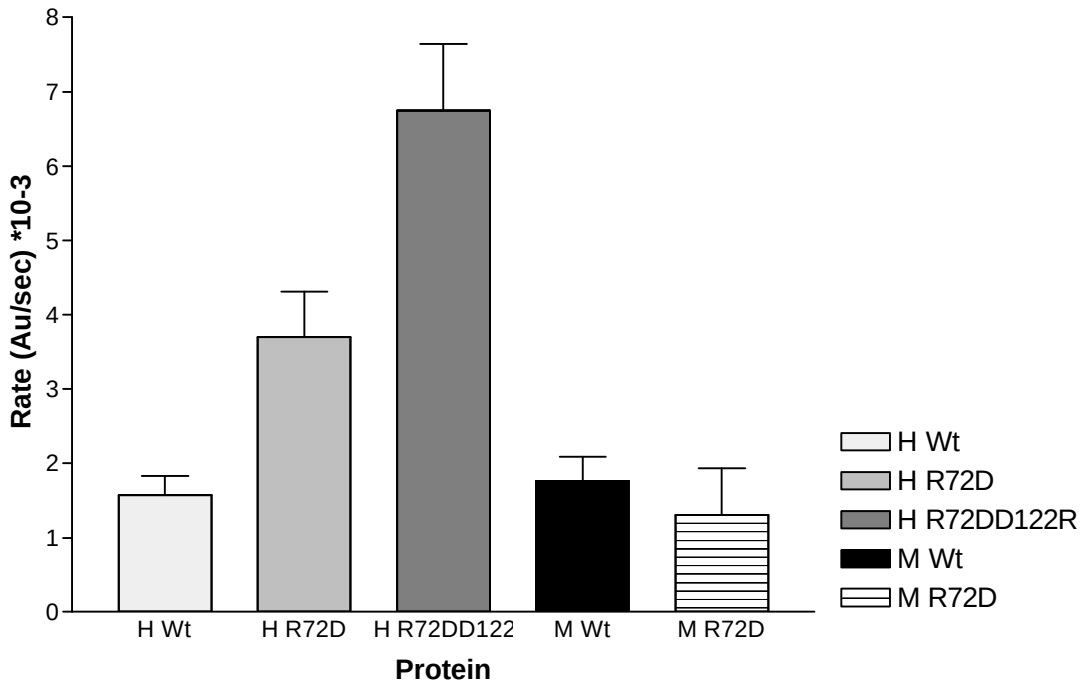

Fig 4. Iron release rates (ÄAu/sec) of various recombinant apoferritins. The error of the initial rates (Ä Au/sec) is the standard deviation of the mean. Initial iron ratio of 480Fe/ferritin: H-wt, 1.570 +/- 0.26; H R72D, 3.69 +/- 0.61, H R72DD122R, 6.75 +/- 0.89; M-wt, 1.76 +/- 0.32 ; M R72D, 1.30 +/- 0.62.

Percentage of iron released after 10 minutes by H-wt, M-wt and mutants

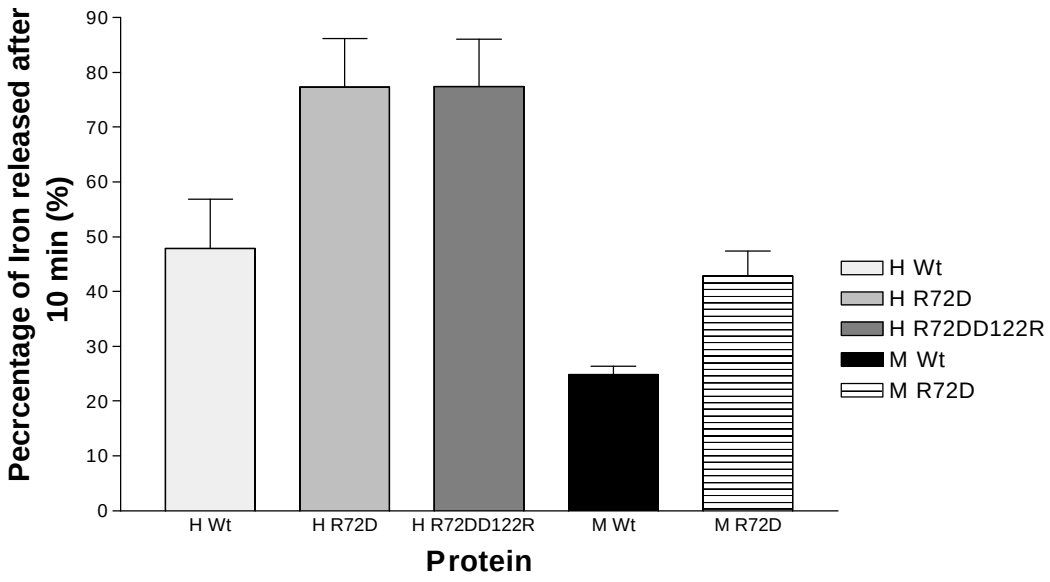

Fig 5 A . Percentage of iron released after 10 minutes for H, M wild type and mutants. Recombinant apoferritins mineralized *in vitro* by mixing with ferrous sulfate at a ratio of 480 Fe/ferritin in 0.1 MOPS (pH 7.0), 0.2 M NaCl and incubated at room temperature for 2 hours and then at 4 ^{o}C overnight were added to a mixture of 2.5 M FNM, 2.5 M NADH and 2.5 M Bipyridyl. Reduced iron was trapped as a Fe(II)-bipyridyl complex monitored at 522 nm. The percentage of iron released was calculated by determining the amount of iron released at 10 minutes and extrapolating a percentage amount from 480 Fe atoms as 100%. The error of the percentage of iron released (%) is the standard deviation of the mean. H-wt, 47.85+/-9.04; H R72D, 77.30+/-8.95; H R72DD122R, 77.37 +/- 8.77; M-wt 24.87 +/- 1.46; M R72D, 42.80 +/- 4.66.

Percentage of iron released after 40 minutes

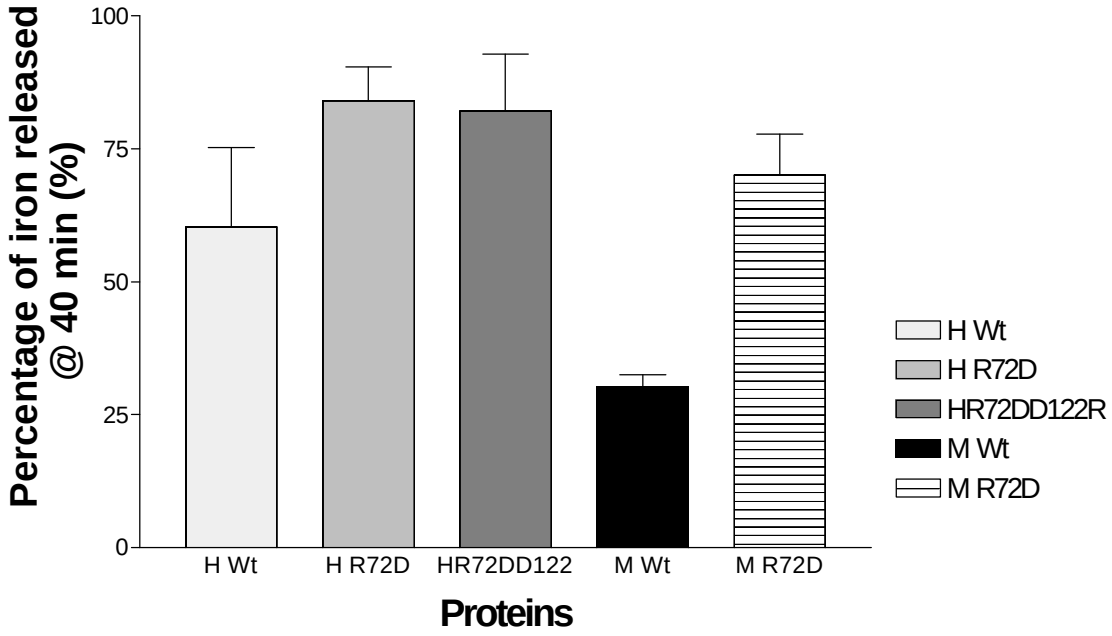

Fig 5B. Percentage of iron released after 40 minutes. H-wt, 60.282 +/-14.90; H R72D,83.96+/-6.48; H R72DD122R, 82.10+/-10.639; M-wt, 30.21 +/-2.30; M R72D,70.08 +/-7.66.

Three fold interface with salt-bridge and area disrupted by the L134P mutation

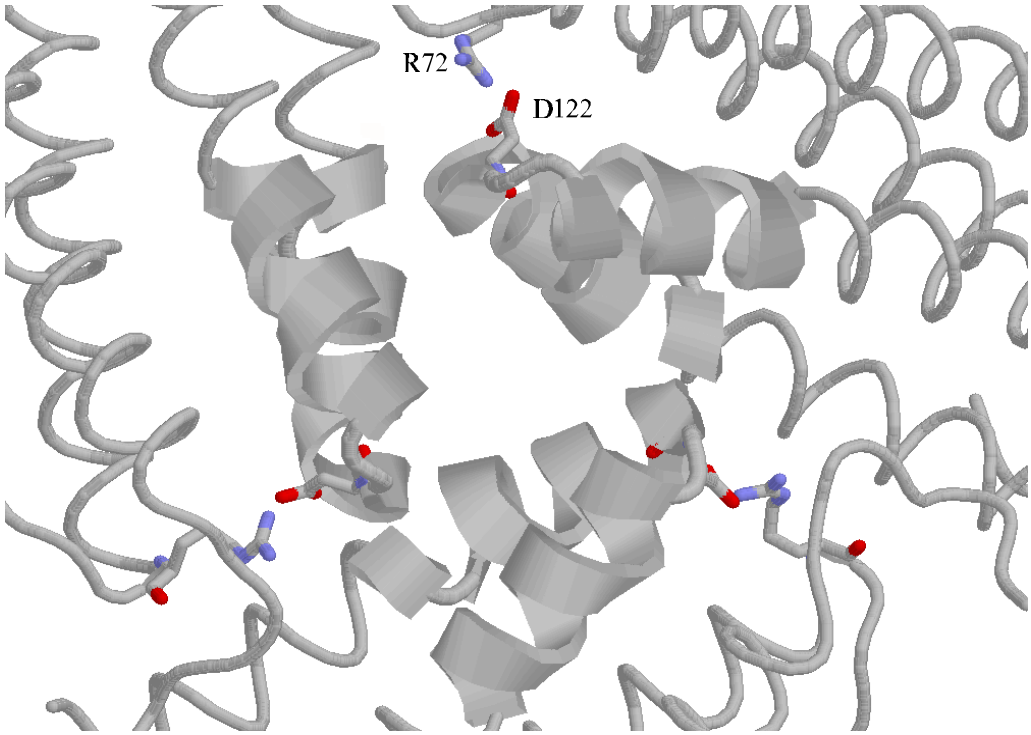

Fig 6. Three fold interface of frog M ferritin. Figure shows the position of the alpha helix disrupted by the L134P mutation (gray ribbon) and the position of the salt bridge between R72 and D122. Prediction of the disrupted C and D helix terminus from Takagi et al 1999. (Drawing produced by Rasmol.)

Elution time at 10 ºC

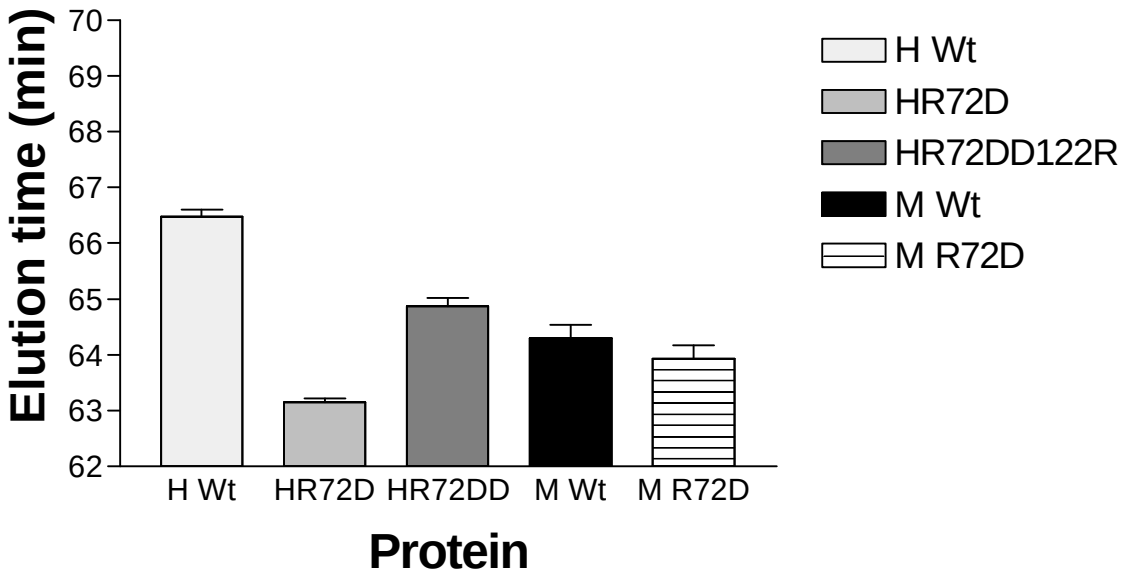

Fig 7A. Gel filtration elution times at 10 ºC (A), 23 ºC (B) and 45.5 ºC (C) for several recombinant apoferritins. Ferritin samples (1.4 mg or less) were injected in a Sepahcryl S-300 (Pharmacia) gel filtration analytical column, and the elution time for the different proteins was determined by measuring the absorption of eluted fractions at 280 nm. The error of the elution times (min) is the standard deviation of the mean. (A) H-wt, 66.47 +/- 0.13; H R72D, 63.15 +/- 0.07; H R72DD122R, 64.87 +/- 0.14; M-wt, 64.29 +/- 0.24; M R72D, 63.93 +/- 0.22.

Elution time at 23 ºC

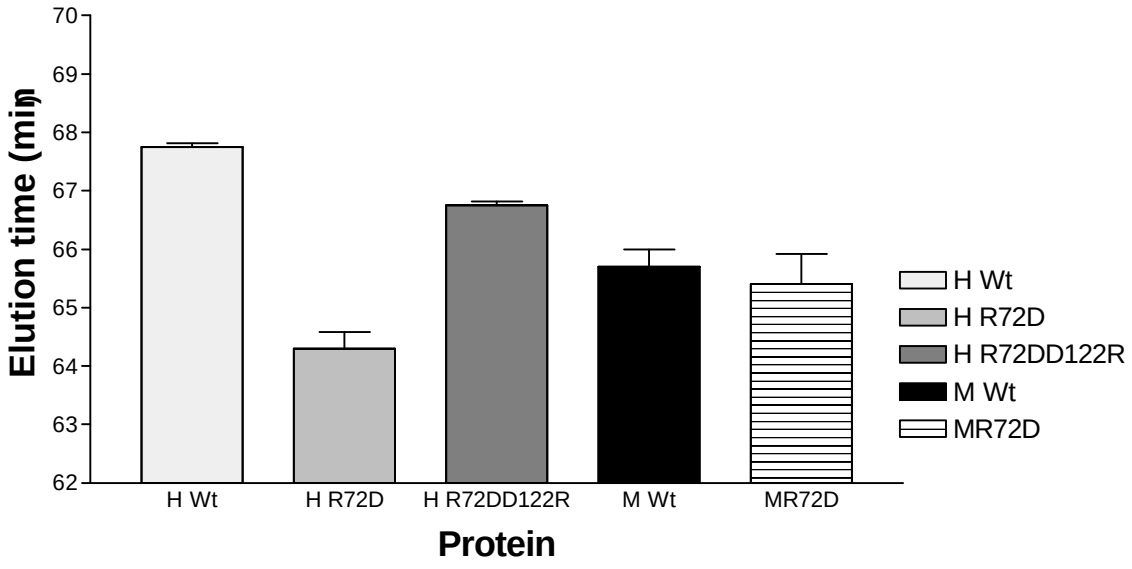

Fig7B. Gel filtration elution times at 23 ºC. H-wt, 67.75 +/- 0.07; H R72D, 64.30 +/- 0.28; H R72DD122R, 66.75 +/-0.07; M-wt, 65.70 +/- 0.29; M R72D, 65.40 +/- 0.51.

Elution time at 45.5 ºC

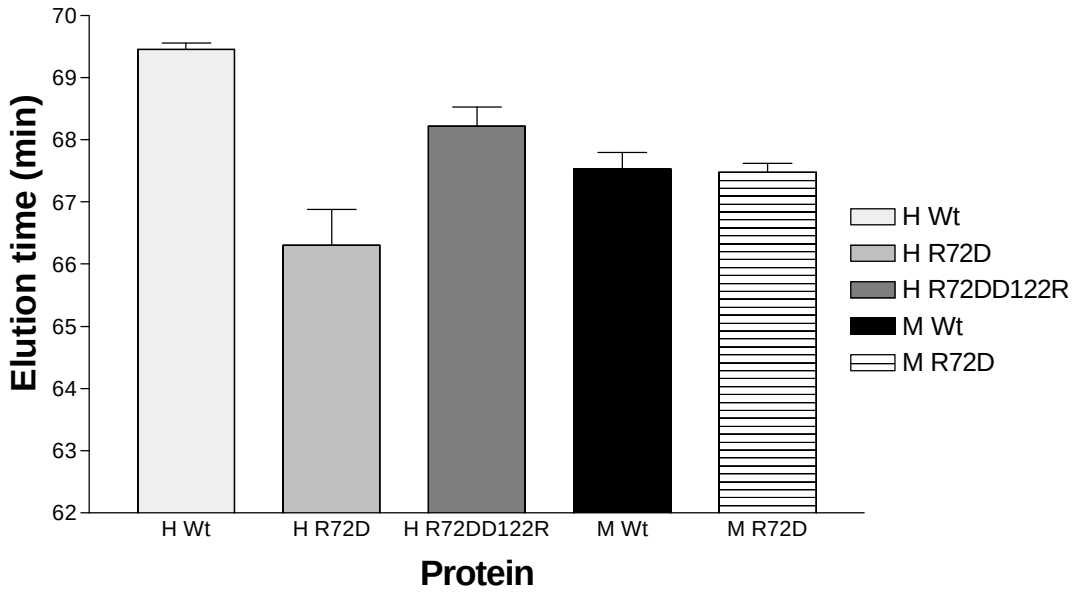

Fig 7C. Gel filtration elution times at 45.5 ºC. H-wt, 69.45 +/- 0.10; H R72D, 66.30 +/- 0.57; H R72DD122R, 68.21 +/- 0.30; M-wt, 67.52 +/- 0.26; M R72D, 67.47 +/- 0.13.

Interactions between the A-B and C-D helix bundle in Frog M ferritin

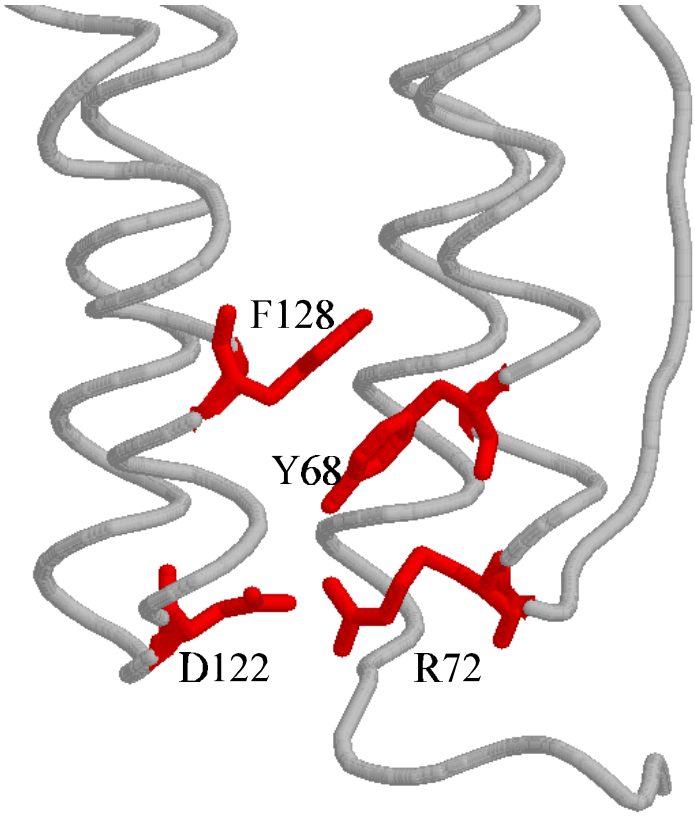

Fig 8. Alpha-Carbon trace drawing of frog M ferritin showing the 3-fold end terminus of the AB-CD helix bundle. Also depicted is the hydrophobic interaction between Y68 and P128 found in frog M ferritin but not in frog H ferritin where the tyrosine 68 residue is replaced by an aspartate. This interaction could provide additional stability to the region in the absence of the R72-D122 salt bridge. (Drawing produced by Rasmol.)

Inter-subunit hydrophobic interactions in human H and frog M ferritin

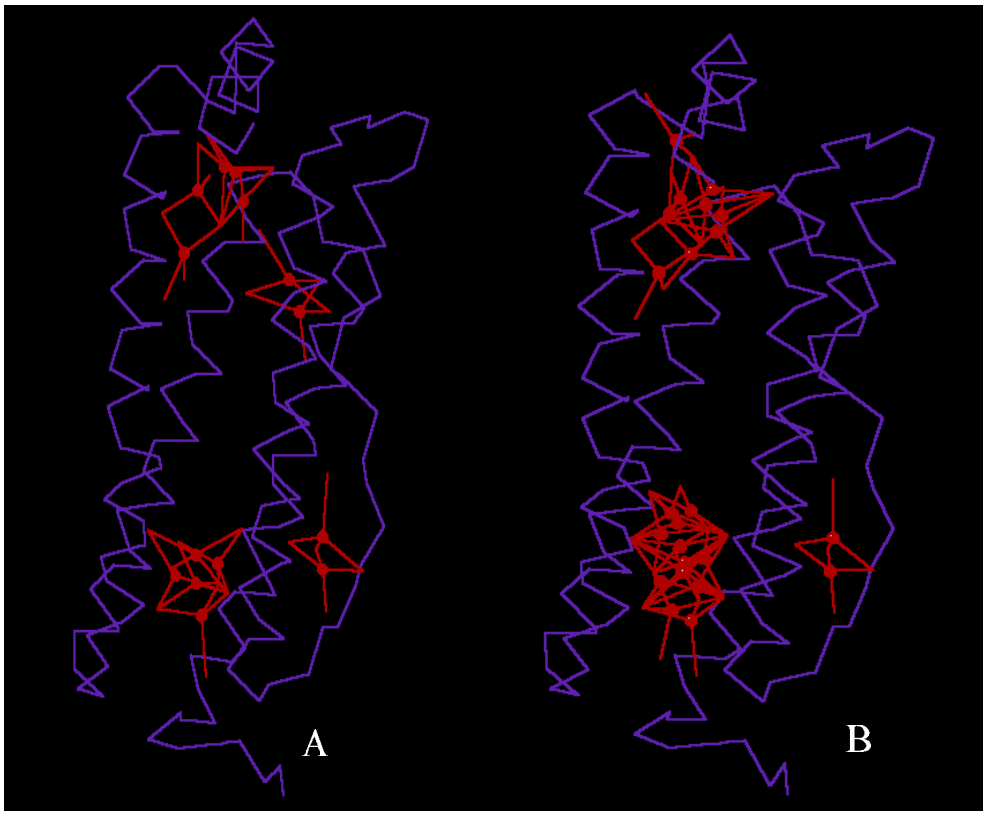

Figure 9. Inter-subunit hydrophobic interactions in human H (A) and frog M (B) ferritin single subunit based on the program ProCam [13]. Red dots represent the interaction center between 4 hydrophobic amino acids. Red lines show the position of the amino acid responsible for the interaction. Specific residues involved in the interaction are not shown for clarity, but the residues involved in the 3-fold terminus of the AB-CD helix bundle are shown in table 4.

Elution time vs Iron uptake rate

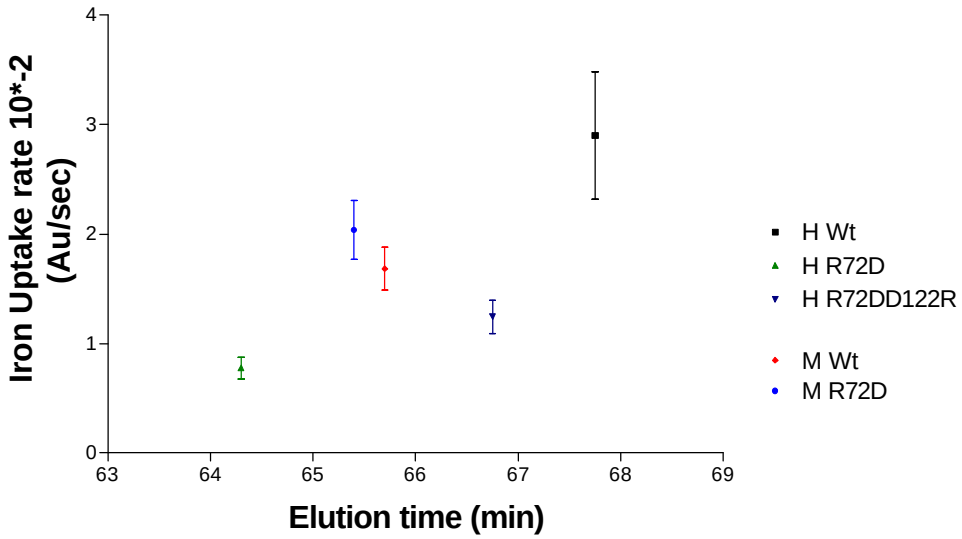

Fig 10. Elution time vs iron uptake rates for several recombinant apoferritins. Elution times at 23 ºC for several recombinant apoferritins were plotted against their iron uptake rate (measured at 350 nm). Standard deviation of the mean of the iron uptake shown by bars. Not shown are the standard deviation in minutes for the elution time of H-wt (0.07), H R72D (0.28), H R72DD122R (0.07), M-wt (0.29), and MR72D (0.51).